Kragujevac J. Sci. 39 (2017) 109-122. UDC 541.127:547.587.52

ANTIOXIDATIVE ACTIVITY OF CAFFEIC ACID – MECHANISTIC DFT STUDY

Izudin Redžepović, Svetlana Marković*, Jelena Tošović

University of Kragujevac, Faculty of Science, Department of Chemistry, Radoja Domanovića 12, 34000 Kragujevac, Republic of Serbia
***Corresponding author; E-mail: mark@kg.ac.rs

(Received March 29, 2017; Accepted April 7, 2017)

ABSTRACT. This paper reports the results of comprehensive mechanistic investigations of the hydrogen atom transfer (HAT), radical adduct formation (RAF), single electron transfer – proton transfer (SET-PT), and sequential proton loss electron transfer (SPLET) mechanisms of caffeic acid (**CA**). The goals of the work were achieved by simulating the reactions of **CA** with hydroxyl radical in benzene and water solutions. It was found that SET-PT is not a favourable antioxidative mechanism of **CA**. On the other hand, HAT and RAF are competitive, because HAT pathways yield thermodynamically more stable radical products, and RAF pathways require smaller activation barriers. In polar basic environment SPLET is a probable antioxidative mechanism of **CA**, with exceptionally large rate.

Key words: activation energies, reaction energies, rate constants, M06-2X/6-311++G(d,p) theoretical model, CPCM solvation model

INTRODUCTION

Phenolic compounds are well-known for their antioxidative action that can be realized via several mechanisms (TRUHLAR *et al.*, 1983; GALANO *et al.*, 2006; KLEIN *et al.*, 2007; LITWINIENKO and INGOLD, 2007: GALANO and ALVAREZ-IDABOY, 2013). The hydrogen atom transfer [HAT, Eq. (1)], radical adduct formation [RAF, Eq. (2)], single electron transfer – proton transfer [SET-PT, Eqs. (3) and (4)], and sequential proton loss electron transfer [SPLET, Eqs. (5) – (7)] mechanisms in caffeic acid (**CA**, Fig. 1) are in the focus of this work:

$$\mathbf{CA} + R^{\bullet} \rightarrow \mathbf{CA}^{\bullet} + RH \quad (1)$$
$$\mathbf{CA} + R^{\bullet} \rightarrow \mathbf{CA\text{-}R}^{\bullet} \quad (2)$$
$$\mathbf{CA} + R^{\bullet} \leftrightarrows \mathbf{CA}^{+\bullet} + R^{-} \quad (3)$$
$$\mathbf{CA}^{+\bullet} + R^{-} \rightarrow \mathbf{CA}^{\bullet} + RH \quad (4)$$
$$\mathbf{CA} + B^{-} \rightarrow \mathbf{CA}^{-} + BH \quad (5)$$
$$\mathbf{CA}^{-} + R^{\bullet} \rightarrow \mathbf{CA}^{\bullet} + R^{-} \quad (6)$$
$$\mathbf{CA} + R^{-} \rightarrow \mathbf{CA}^{-} + RH \quad (7)$$

In Eqs. (1) – (7) $\mathbf{CA}^{\bullet}$, $\mathbf{CA\text{-}R}^{\bullet}$, $\mathbf{CA}^{+\bullet}$, and $\mathbf{CA}^{-}$ represent the radical, radical adduct, radical cation, and anion, respectively, of the parent compound **CA**; while $R^{\bullet}$ and R^{-} stand for a

present free radical and corresponding anion. B^- in Eq. (5) denotes a base whose presence is necessary for heterolytic cleavage of the O–H bonds to occur.

Hydroxycinnamic acids are the most widely distributed phenolic acids in plant kingdom. They are often encountered as glucose and quinic acid esters. As for **CA**, its most abundant conjugate is chlorogenic acid. **CA** exhibits various biological and pharmacological properties, such as anticancerogenic, anti-inflammatory, immunomodulatory, and antiviral activities (CHALLIS and BARTLETT, 1975; FRANK *et al.*, 1989; IWAHASHI *et al.*, 1990; JOYEUX *et al.*, 1995). Many such beneficial features of this antioxidant are related to its ability to inhibit oxidative stress and associated molecular damage (SUDINA *et al.*, 1993; GEBHARDT and FAUSEL, 1997).

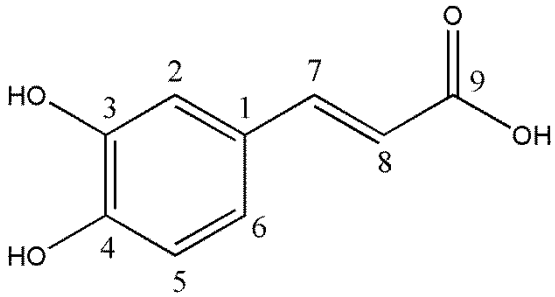

Figure 1. Structural formula of caffeic acid. The atom labelling scheme is remained throughout the text.

A comparative computational study of the antioxidative activities of caffeic and caffeoylquinic acids has been recently carried out by focusing on the thermodynamics of the HAT, SPLET, and SET-PT mechanisms (MARKOVIĆ and TOŠOVIĆ, 2016). It has been revealed that all four acids are characterized with very similar values of the corresponding reaction enthalpies, thus indicating that antioxidative activity of these acids does not depend on the esterification position. This finding complements the results of different experimental assays (XU *et al.*, 2012). It has been put forward that HAT may be the major mechanism in nonpolar media, while HAT and SPLET are competitive pathways in polar environment (MARKOVIĆ and TOŠOVIĆ, 2016). One can assume, based on the fact that **CA** contains a conjugated chain attached to the aromatic ring, that this compound can undergo the RAF antioxidative pathway with small free radicals (LEOPOLDINI *et al.*, 2011).

In spite of the fact that antioxidative activity of **CA** has been the subject of few theoretical investigations (GONZÁLEZ MOA *et al.*, 2006; LITWINIENKO and INGOLD, 2007), the mechanisms of antioxidative action of this important food ingredient have not been fully clarified. The aim of the present paper is to contribute to the explanation of antioxidative activity of **CA** by examining its HAT, RAF, SPLET, and SET-PT reaction pathways in the presence of hydroxyl radical.

THEORETICAL

Numerous theoretical models have become valuable tools in researches related to the antioxidative activity of numerous classes of compounds. In our recent work (MARKOVIĆ and TOŠOVIĆ, 2016), the M06-2X functional (ZHAO and TRUHLAR, 2008) in combination with the 6-311++G(d,p) basis set and CPCM polarizable continuum solvation model (COSSI *et al.*, 2003), has demonstrated robustness and very good overall performance in the investigations of the related problems. Bearing this fact in mind, exactly the same theoretical model was used for all calculations within this work. All computations were carried out by means of the Gaussian 09 software package (FRISCH *et al.*, 2013).

All participants in the investigated reactions were fully optimized in benzene (dielectric constant ε = 2.2706) and water (ε = 78.3553). The restricted and unrestricted calculation schemes were applied for the closed-shell and open-shell systems. The frequency calculations were performed, and the results obtained were used to determine the nature of the revealed stationary points: no imaginary vibrations for equilibrium geometries, and exactly one imaginary vibration for transition states. The relative free energy and enthalpy values were calculated at T = 298.15 K.

Calculating the rate constants

Our study includes both kinetic and thermodynamic approaches to the investigation of the HAT, RAF, SET-PT, and SPLET mechanisms in **CA**. The task was realized by simulating the reactions (1) – (7) of **CA** with hydroxyl radical ($HO^{\bullet}$) in nonpolar (benzene) and polar (water) environments. $HO^{\bullet}$ was selected for its biological significance (BELITZ *et al.*, 2009).

The investigation was divided into two tasks: the one where TS exists between the reactants and products [HAT and RAF, Eqs. (1) and (2)], and the other where there is no TS between the reactants and products [SET-PT and SPLET, Eqs. (3) – (7)]. In all cases, the starting point for calculating the rate constants was the Eyring equation (EVANS and POLANYI, 1935; EYRING, 1935; TRUHLAR *et al.*, 1983). In contemporary solution phase kinetics, this equation turned out to be the most straightforward way to interpret temperature dependence of rate constants (LENTE, 2015):

$$k = \frac{\mathrm{k_B}T}{\mathrm{h}} \exp\left(-\Delta G_{\mathrm{a}}^{\ddagger} / \mathrm{R}T\right) \tag{10}$$

In Eq. (10) h and $\mathrm{k_B}$ denote the Planck and Boltzmann constants, and $\Delta G_{\mathrm{a}}^{\ddagger}$ is the free activation energy. Dimensional analysis of Eq. (10) shows that it yields the first order rate constant, that is valid for unimolecular reactions. It is a common practice to use the Eyring equation for calculating bimolecular rate constants too. Namely, the two reactants are assumed to form RC, and the process is considered as a unimolecular reaction of this RC. Then, the second order rate constant is given as:

$$k_{\mathrm{bim}} = \frac{\mathrm{k_B}T}{\mathrm{c}^{\ominus}\mathrm{h}} \exp\left(-\Delta G_{\mathrm{a}}^{\ddagger} / \mathrm{R}T\right) \tag{11}$$

where $\mathrm{c}^{\ominus} = 1\mathrm{M}$ concentration by usual convention. Eq. (11) was used to calculate the rate constants for the HAT and RAF antioxidative pathways [reactions (1) and (2)].

In the case of the SET-PT and SPLET mechanisms the Marcus theory (MARCUS, 1993; MILENKOVIĆ *et al.*, 2016) was used to estimate the activation barriers for the electron transfer (ET) reactions (3) and (6):

$$\Delta G_{\mathrm{aET}}^{\ddagger} = \frac{\lambda}{4}\left(1 + \frac{\Delta G_{\mathrm{r}}}{\lambda}\right)^2 \tag{12}$$

In Eq. (12) ΔG_{r} and λ denote the reaction free energy and reorganization energy. λ was estimated as follows (NELSEN *et al.*, 1987; NELSEN *et al.*, 2006; MARTÍNEZ *et al.*, 2012):

$$\lambda \approx \Delta E - \Delta G_{\mathrm{r}} \tag{13}$$

where ΔE is the non-adiabatic difference in total energy between the vertical products and reactants. Some rate constants obtained by inserting Eq. (12) into Eq. (10) were close to the diffusion limit. For this reason, the apparent rate constants (k_{app}) were obtained using the Collins-Kimball theory (COLLINS and KIMBALL, 1949):

$$k_{\mathrm{app}} = \frac{k_{\mathrm{D}} k}{k_{\mathrm{D}} + k} \tag{14}$$

where k_D stands for the diffusion rate constant. The main assumption in the Collins-Kimball theory is that reaction takes place at a specific distance α. This distance was calculated as the sum of the reactants radii: $\alpha = \alpha_{\mathbf{CA}} + \alpha_{\mathrm{HO}\bullet}$ [Eq. (3)]; $\alpha = \alpha_{\mathbf{CA}^-} + \alpha_{\mathrm{HO}\bullet}$ [Eq. (6)]. The Collins-Kimball theory relies on the assumption of Smoluchowski, implying that molecules are treated as non-overlapping spheres that diffuse as Brownian particles with diffusion rate k_D. Then, the steady state SMOLUCHOWSKI (1917) rate constant for an irreversible bimolecular diffusion controlled reaction is defined as:

$$k_{\mathrm{D}} = 4\pi\alpha D \mathrm{N}_{\mathrm{A}} \tag{15}$$

In Eq. (15) N_A denotes the Avogadro number, and D is the mutual diffusion coefficient of the reactants. According to the Truhlar assumption the motion of two molecular species is considered as the motion of free radical ($HO^\bullet$ in our case) that diffuse with respect to the other particle (**CA** or $\mathbf{CA^-}$) (TRUHLAR, 1985). Then, D can be calculated using the Stokes-Einstein approach (STOKES, 1901; EINSTEIN, 1905) as the sum of the corresponding diffusion coefficients:

$$D_{\mathbf{CA}} = \frac{k_{\mathrm{B}}T}{6\pi\eta\alpha_{\mathbf{CA}}} \quad D_{\mathbf{CA}^-} = \frac{k_{\mathrm{B}}T}{6\pi\eta\alpha_{\mathbf{CA}-}} \quad D_{\mathrm{HO}\bullet} = \frac{k_{\mathrm{B}}T}{6\pi\eta\alpha_{\mathrm{HO}\bullet}} \tag{16}$$

where η represents the solvent viscosity [$\eta = 0.6028\times10^{-3}$ and 0.8905×10^{-3} Pa·s for benzene and water (http://www.trimen.pl/witek/ciecze/liquids.html)].

RESULTS AND DISCUSSION

HAT mechanism

As already mentioned, the HAT mechanism is regarded as direct hydrogen atom transfer from phenolic groups of **CA** to $HO^\bullet$. **CA** and $HO^\bullet$ can build two RCs: **RC3** and **RC4**. These RCs pass through **TS3** and **TS4**, and eventually yield **PC3** and **PC4**. Each PC consists of water molecule and corresponding **CA** radical (**CA3**$^\bullet$ and **CA4**$^\bullet$). The so-obtained free radicals are far less reactive in comparison to $HO^\bullet$. The structures of RCs, TSs, and PCs figuring in the HAT pathways of **CA** are depicted in Fig. 2, whereas bond evolution is presented in Table 1.

Table 1 shows that the O10–H3 and O10–H4 distances in corresponding RCs are significantly shorter in benzene than in water. Actually, deviation of the $HO^\bullet$ moiety from the RC plane is not pronounced in benzene (Fig. 2), whereas it is positioned "above" the ring in water. This occurrence is, certainly, a consequence of different polarity of the two solvents. As the reaction occurs, the O3–H3 and O4–H4 distances increase (indicating cleavage of bonds), the C3–O3 and C4–O4 distances decrease (indicating transformation of single into double bonds), and the O10–H3 and O10–H4 distances decrease (indicating formation of water molecule).

Variation of enthalpy and free energy along the reaction coordinate in the 3 and 4 positions is depicted in Fig. 3. Behaviour of each energy follows very similar trends in water and benzene solutions. When enthalpy is considered, RC lies lower than the reactants because of the optimal Van der Waals and Coulomb interactions. On the other hand, RC lies higher than the reactants in the free energy curve, due to the negative entropy change caused by increased amount of order. In the further course of the reaction, both enthalpy and free energy increase up to TS, and fast decrease down to PC. Then, Gibbs energy continues to decrease

(positive entropy change because of reduced amount of order), whereas enthalpy slightly increases up to the products (no intermolecular interaction between separated **CA•** and water molecule).

Table 1. Crucial interatomic distances along the reaction coordinate in the HAT pathways of caffeic acid with hydroxyl radical. The oxygen of hydroxyl moiety is labelled O10.

	Distance (pm)	Water			Benzene		
		RC	TS	PC	RC	TS	PC
Pathway 3	O3–H3	96.4	103.2	200.0	96.7	103.9	196.1
	O10–H3	358.7	154.2	96.8	209.3	150.5	96.8
	O3–C3	135.9	134.1	125.0	136.5	133.8	124.9
	C3–C4	140.9	143.7	146.9	140.6	143.6	146.9
	C3–C2	138.2	139.1	143.8	138.4	139.3	143.9
Pathway 4	O4–H4	96.3	103.2	204.5	96.8	104.1	198.7
	O10–H4	354.4	152.8	96.7	204.2	148.8	96.7
	O4–C4	135.5	133.6	124.3	136.1	133.3	124.2
	C4–C3	140.8	143.5	147.4	140.5	143.3	147.4
	C4–C5	138.8	140.3	144.6	138.8	140.3	144.6

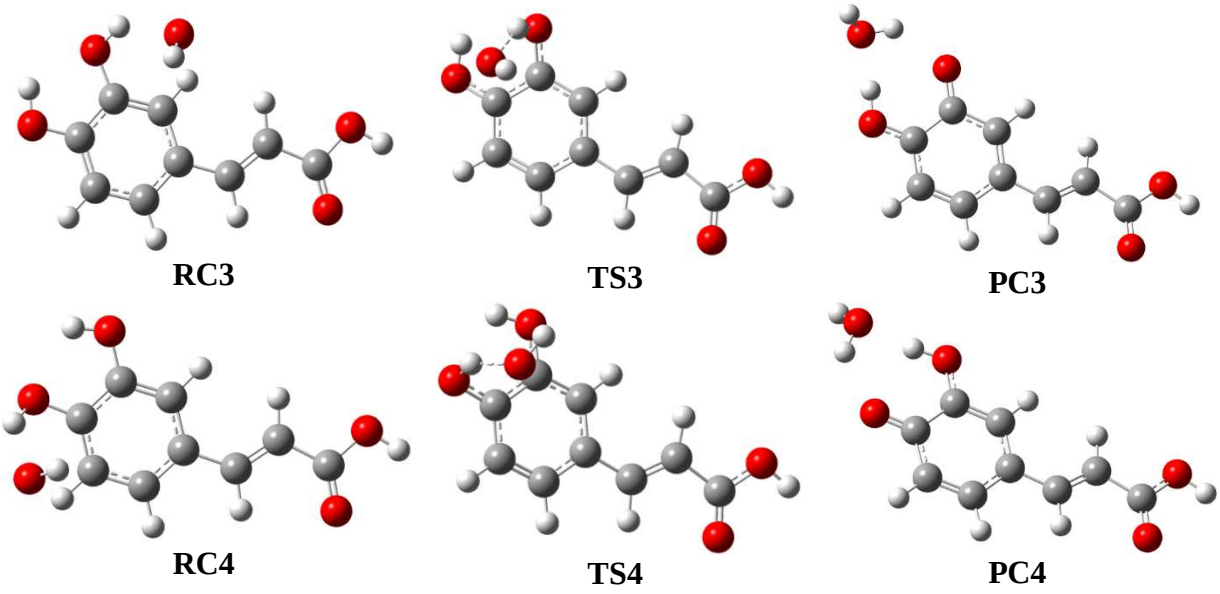

Figure 2. Characteristic stationary points in the HAT pathways of caffeic acid with hydroxyl radical.

Reaction energetics and corresponding rate constants are collected in Table 2. The reactions in both 3 and 4 positions are noticeably exothermic and exergonic. As expected, the activation energies and corresponding rate constants slightly depend on the solvent polarity. The k_{bim} values for pathway 3 are slightly larger than those for pathway 4 in both solvents. However, **CA4•** is more stable than **CA3•** (Table 2). In accord with this finding are the spin density surfaces of the two free radicals (Fig. 4). These surfaces reveal that the unpaired electron in **CA3•** is delocalized over the benzene ring, whereas in **CA4•** it is delocalized over the ring and conjugated chain.

One can conclude, on the basis of the kinetic and thermodynamic analysis of the two HAT pathways, that both reaction paths are favourable in nonpolar and polar solvents. Small differences in activation energies (rate constants) and stabilities of the yielded **CA•** radicals make these two reaction paths competitive.

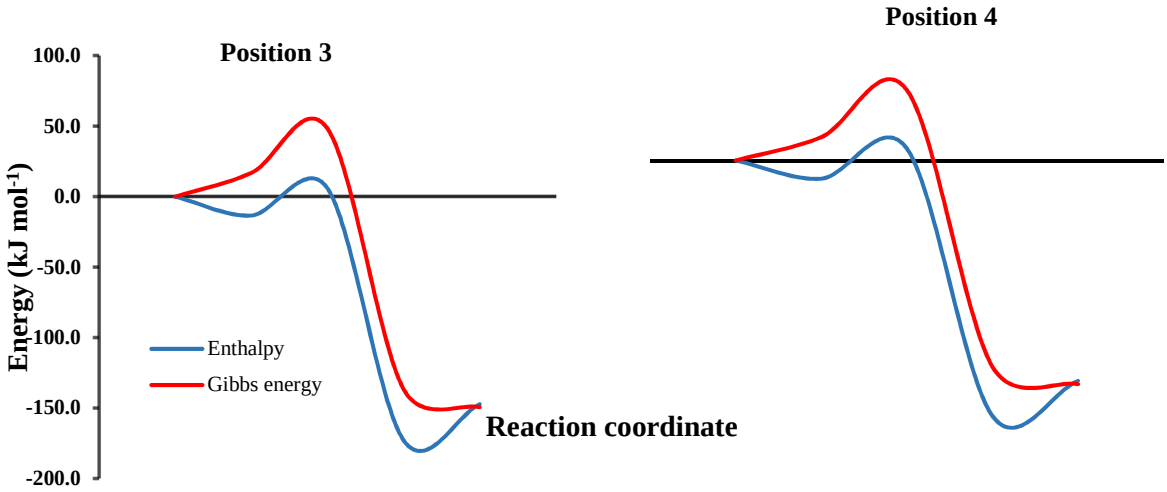

Figure 3. Energy profiles for the HAT pathways of caffeic acid with hydroxyl radical in water solution.

Table 2. Enthalpy (*italic*) and free energy (regular) values along the reaction coordinate in the HAT pathways of caffeic acid with hydroxyl radical. The energies were calculated relative to those of separated reactants. k_{bim} stands for the corresponding rate constants.

Position	**RC** kJ mol^{-1}	**TS** kJ mol^{-1}	**PC** kJ mol^{-1}	**products** kJ mol^{-1}	$\Delta G_a^{\ddagger}$ kJ mol^{-1}	k_{bim} M^{-1} s^{-1}
			W a t e r			
3	*-13.4*	*5.8*	*-173.0*	*-147.3*		
	16.9	48.2	-136.7	-149.4	31.3	2.06×10^{7}
4	*-12.9*	*8.4*	*-181.4*	*-156.5*		
	16.6	50.0	-146.5	-158.9	33.4	0.88×10^{7}
			B e n z e n e			
3	*-19.8*	*0.4*	*-179.1*	*-146.3*		
	15.9	43.4	-141.5	-147.9	27.5	9.46×10^{7}
4	*-17.9*	*3.6*	*-187.4*	*-155.9*		
	15.4	45.3	-151.0	-157.1	29.9	3.54×10^{7}

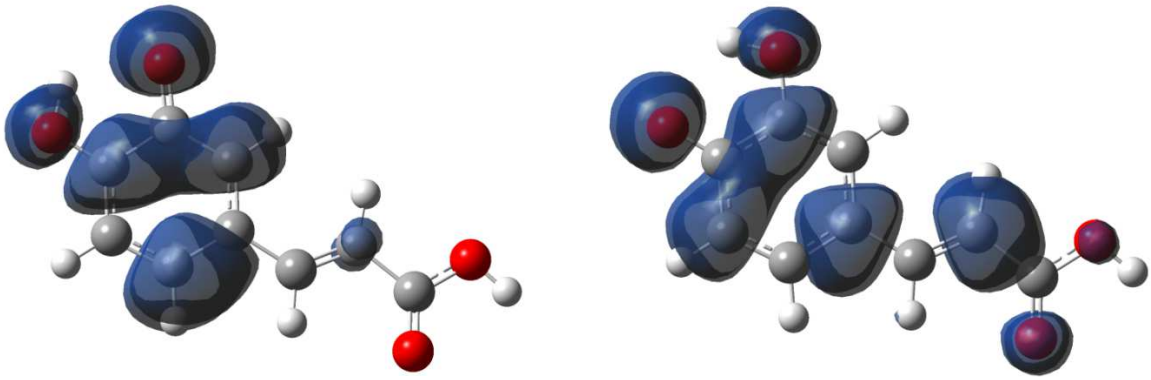

Figure 4. Spin density surfaces for **CA3•** (left) and **CA4•** (right).

RAF mechanism

In a RAF pathway HO• binds to a carbon of **CA**, thus forming a new free radical, called radical adduct. Very similar situation was observed in water and benzene. The reaction also starts with the formation of RCs (Fig. 5). We were only able to reveal **RC4**, **RC6**, and **RC8**. An inspection of the spin density surfaces in these RCs shows that the unpaired electron is delocalized over the hydroxyl moiety and entire caffeic moiety. In **RC4**, **RC6**, and **RC8** spin delocalization includes C3, C4, and C5; C1, C5 and C6; and C7, C8, and C9, respectively, indicating that all these carbons can be attacked by HO•. A vicinity of C2 to the hydroxyl moiety in **RC6** (348.0 and 358.1 pm in water and benzene, Table 3) designates this RC as a stationary point in pathway 2. In the further course of the reaction these RCs pass through TSs where C–O distances become significantly shorter, and in the products the C–O bonds are completely formed (Fig. 5 and Table 3). It is apparent from Fig. 5 that, as the reaction in position 1 progresses, the reaction system becomes non-planar, and therefore, conjugation between the acyclic chain and aromatic ring is lost. Also, addition of HO• to the double C7–C8 bond causes notable deviation of the chain skeleton from the ring plane.

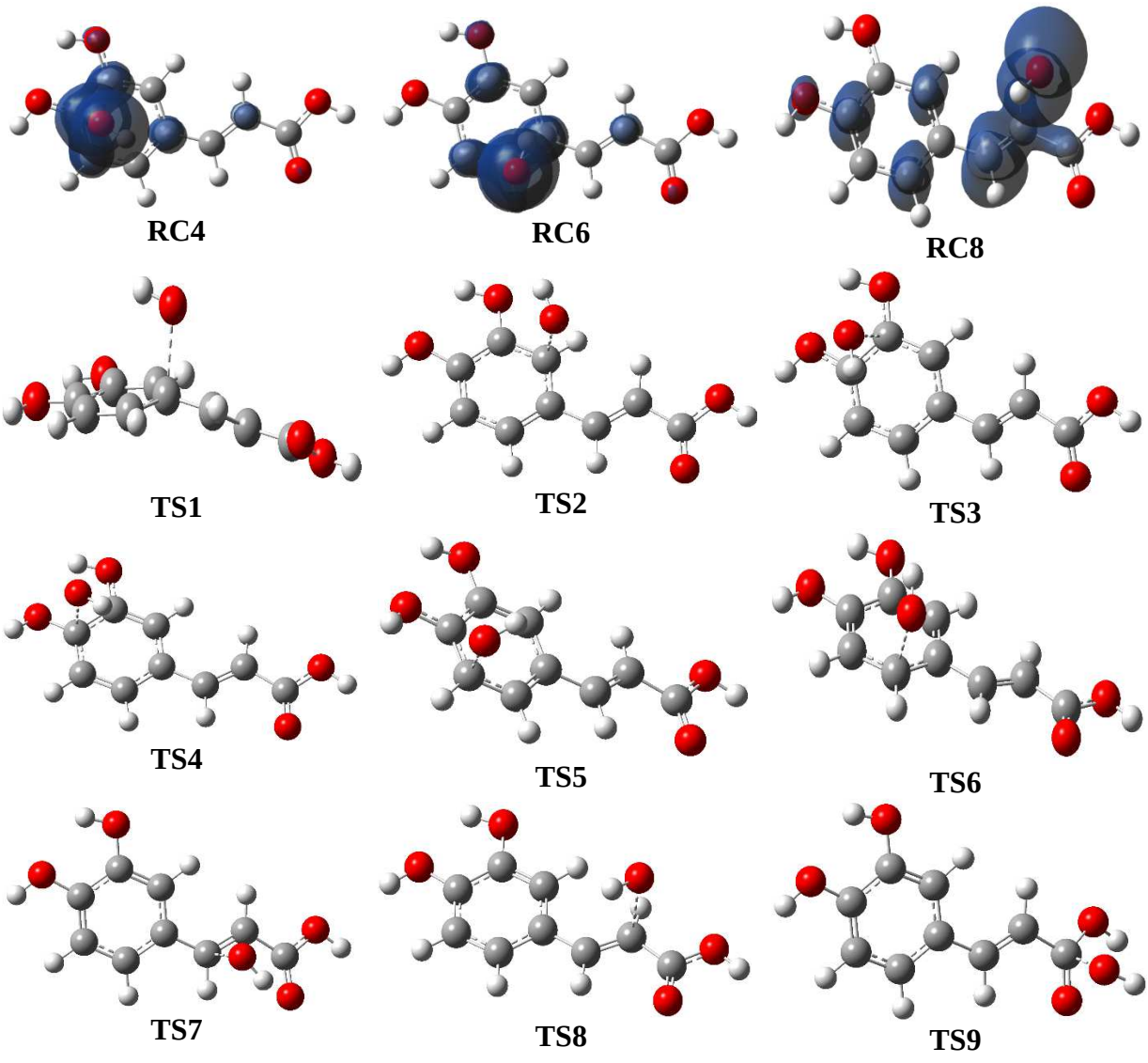

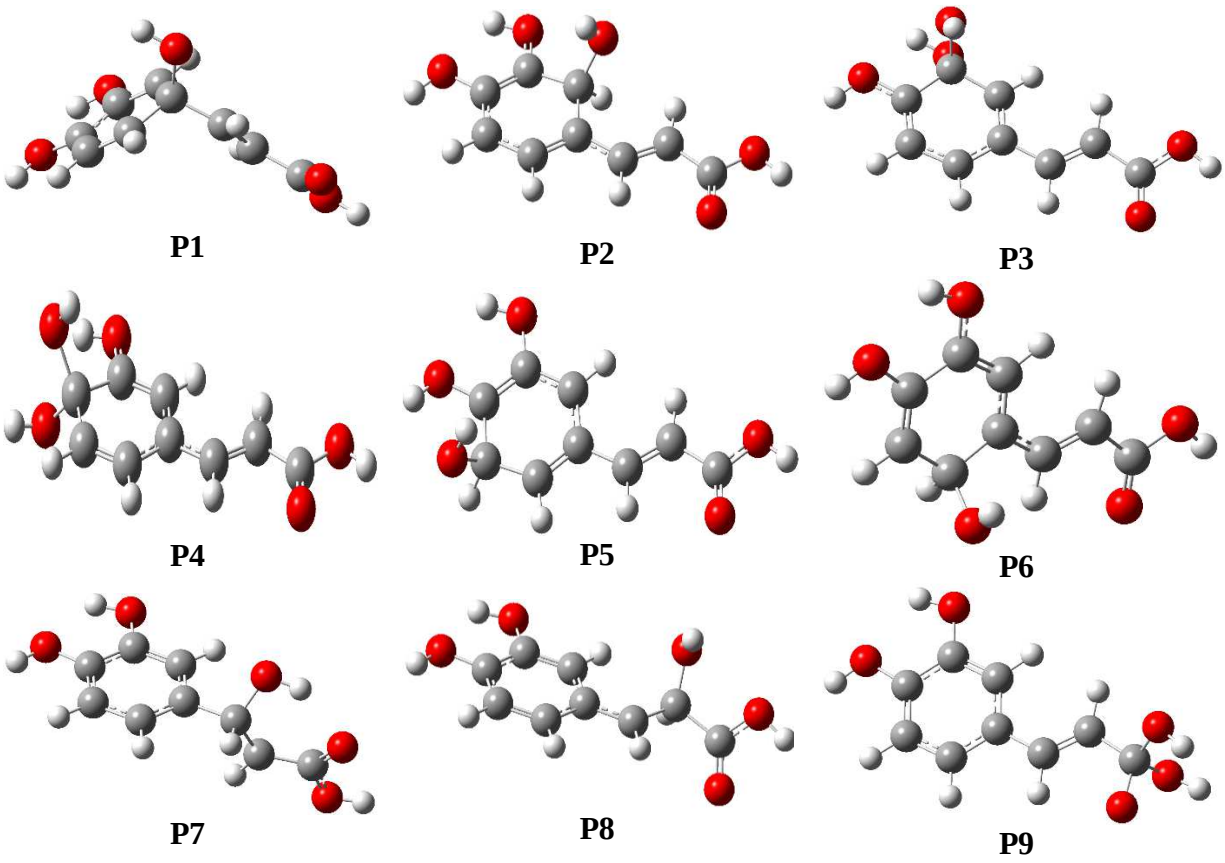

Figure 5. Characteristic stationary points in the RAF pathways of caffeic acid with hydroxyl radical. In **RC4**, **RC6**, and **RC8** spin density surfaces are depicted.

Table 3. Crucial interatomic distances along the reaction coordinate in the RAF pathways of caffeic acid with hydroxyl radical. The oxygen of hydroxyl moiety is labelled O10.

	Distance	**Water**			**Benzene**		
	(pm)	**RC**	**TS**	**P**	**RC**	**TS**	**P**
pathway 1	C1–O10	284.4	203.2	144.4	291.3	200.9	144.0
pathway 2	C2–O10	348.0	143.5	147.4	358.1	208.8	143.2
pathway 3	C3–O10	294.8	211.2	143.2	311.4	206.2	143.1
pathway 4	C4–O10	272.9	220.0	142.4	271.5	219.6	142.6
pathway 5	C5–O10	300.5	205.2	143.7	286.5	203.1	143.7
pathway 6	C6–O10	275.4	133.6	124.3	270.2	209.8	143.4
pathway 7	C7–O10	297.6	212.8	142.1	296.7	210.6	141.6
pathway 8	C8–O10	248.9	226.2	141.6	249.5	220.6	141.9
pathway 9	C9–O10	287.1	180.4	138.9	294.4	180.2	140.3

Variation of enthalpy and free energy along the RAF pathways in water and benzene solutions (Fig. 6) is very similar to that of the HAT pathways. These enthalpy and Gibbs energy changes are quantitatively presented in Table 4. The corresponding rate constants are also collected in Table 4. A comparison of Tables 2 and 4 reveals that, as in the case of the HAT mechanism, RAF pathways are somewhat faster in water than in benzene. In general, RAF pathways are faster in comparison to HAT pathways, but less exothermic and exergonic, and even endothermic and endergonic. In addition, RAF pathways are mutually quite different. As expected, the most favourable sites in **CA** for HO$^{\bullet}$ binding are the carbons of the double bond: C8 and C7. These pathways require the smallest activation energies (show the

largest rate constants, Table 4), and yield the most stable radical adducts. At first glance, some positions in the benzene ring are suitable for addition of HO•. Pathway 4 requires the smallest activation barrier because TS4 is stabilized by the O3–H3···O10 hydrogen bond (Fig. 5). However, this pathway leads to the disturbance of aromaticity, and consequently, to less stable radical adducts (Table 4).

Table 4. Enthalpy (*italic*) and free energy (regular) values along the reaction coordinate in the RAF pathways of caffeic acid with hydroxyl radical. The energies were calculated relative to those of separated reactants. k_{bim} stands for the corresponding rate constants.

Position	RC kJ mol^{-1}	TS kJ mol^{-1}	Products kJ mol^{-1}	$\Delta G_a^{\ddagger}$ kJ mol^{-1}	k_{bim} M^{-1} s^{-1}
			Water		
1	*-11.7* 17.9	*7.4* 50.0	*-59.1* -17.8	*19.1* 32.1	1.48×10^{7}
2	*-12.6* 18.6	*-3.3* 37.0	*-94.1* -49.6	*9.3* 18.4	3.65×10^{9}
3	*-12.9* 18.2	*-3.2* 38.2	*-82.4* -38.7	*9.7* 20.0	1.91×10^{9}
4	*-12.9* 16.6	*-11.0* 31.5	*-115.2* -71.6	*1.9* 14.9	1.54×10^{10}
5	*-13.0* 16.6	*-1.2* 41.0	*-71.1* -27.9	*14.2* 24.4	3.31×10^{8}
6	*-11.9* 17.4	*-3.3* 34.8	*-94.1* -50.1	*8.6* 17.4	5.45×10^{8}
7	*-12.3* 20.3	*-1.1* 41.2	*-122.8* -80.8	*11.2* 20.9	1.33×10^{9}
8	*-12.3* 20.3	*-13.1* 27.3	*-133.5* -90.1	*-0.8* 7.0	3.63×10^{11}
9	*-12.3* 20.3	*60.4* 105.7	*13.2* 58.2	*72.7* 85.4	6.86×10^{-3}
			Benzene		
1	*-13.5* 16.1	*10.3* 52.2	*-60.4* -16.5	*23.8* 36.1	2.91×10^{6}
2	*-13.5* 16.1	*-4.5* 37.1	*-95.2* -51.7	*9.0* 21.0	1.28×10^{9}
3	*-15.3* 10.5	*-1.7* 40.1	*-82.7* -38.6	*13.6* 29.6	3.98×10^{7}
4	*-15.6* 10.5	*-12.6* 29.6	*-119.9* -74.1	*3.0* 19.1	2.82×10^{9}
5	*-15.3* 10.5	*-3.7* 39.0	*-77.4* -33.2	*11.6* 28.5	6.26×10^{7}
6	*-13.5* 16.1	*-2.9* 37.7	*-95.9* -51.6	*10.6* 21.6	1.03×10^{9}
7	*-13.1* 21.3	*-3.0* 39.5	*-127.8* -89.0	*10.1* 18.2	4.04×10^{9}
8	*-13.1* 21.3	*-12.8* 27.9	*-134.8* -91.3	*0.3* 6.6	4.27×10^{11}
9	*-13.1* 21.3	*58.0* 103.1	*10.3* 54.9	*71.1* 81.8	2.84×10^{-2}

Table 4 and Fig. 6 show that C9 is by far the most unfavourable site for binding HO$^{\bullet}$ to **CA**. This finding refers to both kinetic and thermodynamic points of view. This carboxylic carbon is electrophilic, and thus, not susceptible to attack of other electrophilic particles. The second most unfavourable RAF pathway is that in position 1. As stated earlier, this reaction path is followed with significant deviation from planarity (Fig. 5), and thus, disruption of electron delocalization between the benzene ring and acyclic chain.

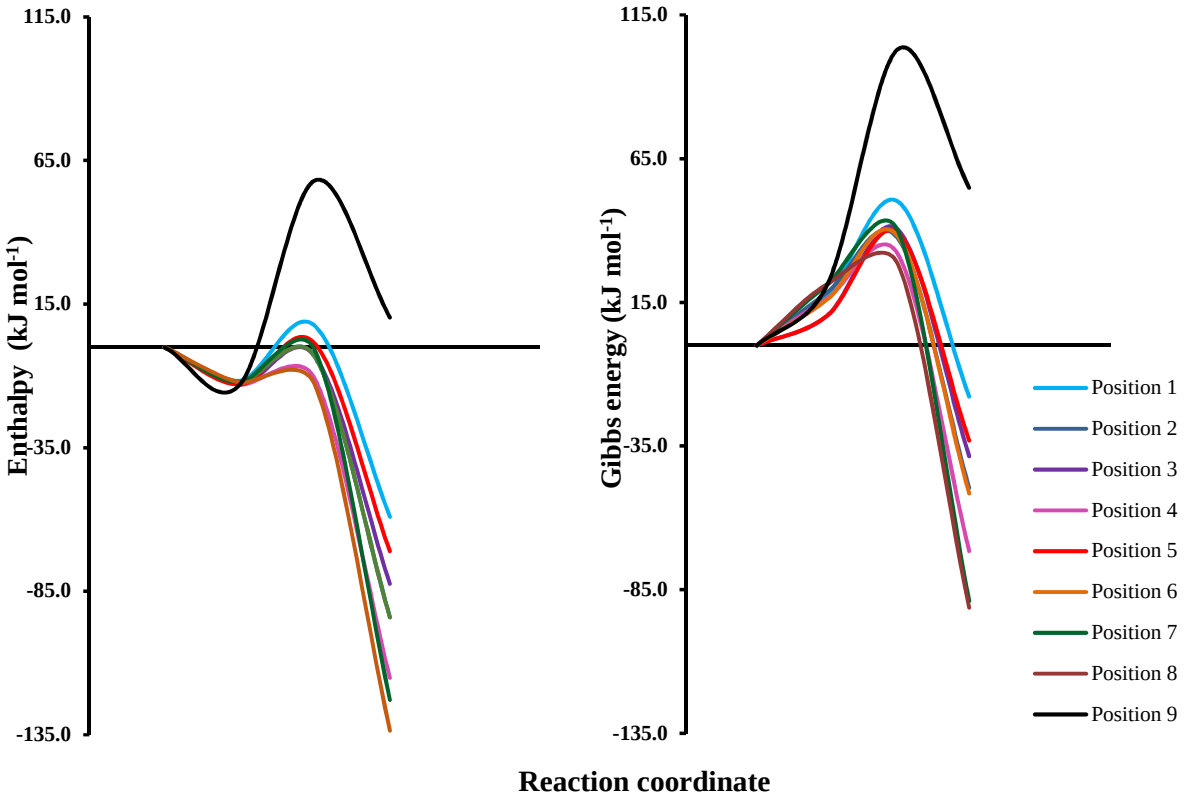

Figure 6. Energy profiles for the RAF pathways of caffeic acid with hydroxyl radical in water solution.

SET-PT and SPLET mechanisms

SET-PT is a two-step antioxidative mechanism. The first step is electron transfer (ET) from **CA** molecule HO$^{\bullet}$ [reaction (3)] where the radical cation of caffeic acid **CA**$^{+\bullet}$ is formed. In the second step **CA**$^{+\bullet}$ donates a proton to the formed base [reaction (4)]. Fig. 7 shows that the unpaired electron is delocalized over the entire radical cation.

Following the above described procedure [Eq. (12)] the activation energies and rate constants were estimated for ET, and the results are summarized in Table 5. It is apparent that the ET reactions are noticeable endergonic, particularly in benzene, and are characterized with enormously large activation barriers. The corresponding rate constants are (practically) equal to zero. These results undoubtedly indicate that the equilibrium in Eq. (3) is completely shifted to the left, implying that reaction (4) cannot take place at all. In other words, SET-PT is not a possible antioxidative pathway of **CA** even with highly electrophilic and reactive free radicals in polar media.

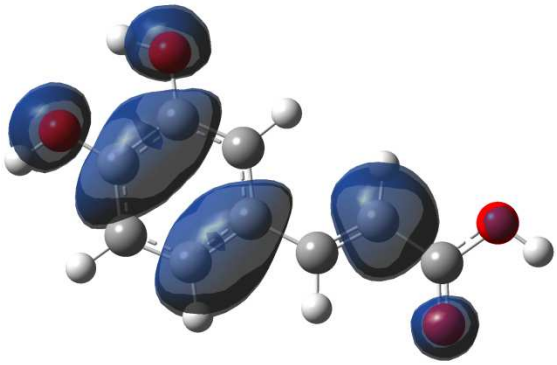

Figure 7. Spin density surface of the radical cation of caffeic acid.

Table 5. Characteristic energies and rate constants in the electron transfer reactions from **CA** to HO•.

	ΔG_r kJ mol^{-1}	λ kJ mol^{-1}	$\Delta G_a^{\ddagger}$ kJ mol^{-1}	k_{bim} M^{-1} s^{-1}
Water	114.6	19.2	232.9	9.85×10^{-29}
Benzene	343.5	1806.0	2149.5	0.00

SPLET is a three-step mechanism. The first step is a heterolytic cleavage of O–H bond in **CA**, which proceeds spontaneously in the presence of a base. Two phenolate anions can be formed as the products of this reaction step: **CA3⁻** and **CA4⁻** (Fig. 8). Certainly, the carboxylate anion is also yielded, but it will not be considered in this work because it does not influence antioxidative activity of **CA**. **CA4⁻** is more stable than **CA3⁻** by 11.4 kJ mol^{-1} (in water) and 15.9 kJ mol^{-1} (in benzene). A comparison of the HOMOs of the two anions reveals that the anionic electron pair is delocalized over the benzene ring in **CA3⁻**, and over the entire molecule in **CA4⁻**.

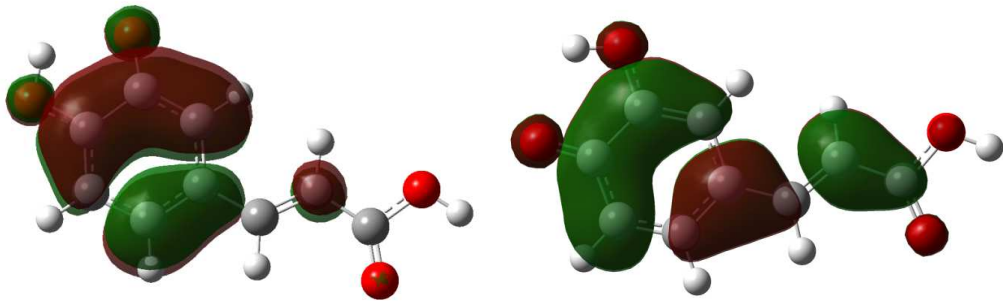

CA3⁻ **CA4⁻**

Figure 8. Phenolate anions of caffeic acid with HOMOs depicted.

The second step of SPLET is ET from **CA⁻** to HO• where **CA•** and HO⁻ are obtained as the products [reaction (6)]. The activation barriers and corresponding rate constants for ET were calculated using the Marcus theory, and the results are summarized in Table 6.
The ΔG_r values reveal that ET reaction in nonpolar benzene is endergonic, whereas in polar water it is exergonic. One can conclude, on the basis of the k_{app} values that ET is much faster in water than in benzene. Both occurrences are the result of stabilization of the formed anions in polar solvent. Identical k_{bim} and k_{app} values show that the ET rate in benzene is far from the rates of diffusion controlled reactions. On the other hand, very similar k_D and k_{app} values in

water indicate that ET is a diffusion controlled reaction in this solvent. In this step the hydroxide anions are generated, and they participate in the third step of the SPLET mechanism [reaction (7)] by propagating the chain reaction. In conclusion, in polar basic environment, SPLET is a plausible antioxidative pathway of **CA** characterized with extremely large rate.

Table 6. Characteristic energies and rate constants in the electron transfer reactions from **CA⁻** to HO•.

	Position	ΔG_r kJ mol^{-1}	λ kJ mol^{-1}	$\Delta G_a^{\ddagger}$ kJ mol^{-1}	k_{bim} M^{-1} s^{-1}	k_D M^{-1} s^{-1}	k_{app} M^{-1} s^{-1}
Water	3	-30.4	16.0	3.2	1.71×10^{12}	7.96×10^{9}	7.92×10^{9}
	4	-28.4	14.5	3.3	1.63×10^{12}	7.98×10^{9}	7.94×10^{9}
Benzene	3	36.4	16.5	42.2	2.32×10^{5}	1.19×10^{10}	2.32×10^{5}
	4	43.1	15.4	34.0	6.85×10^{6}	1.18×10^{10}	6.85×10^{6}

CONCLUSIONS

A systematic investigation of the HAT, RAF, SET-PT, and SPLET antioxidative mechanisms of **CA** was performed, by examining chemical behaviour of **CA** towards HO• in nonpolar (benzene) and polar (water) media. It was found, in accordance with our expectations, that HAT and RAF slightly depend on solvent polarity, whereas SET-PT and SPLET are enabled in water.

The two HAT pathways (3 and 4) are characterized with small differences in activation energies (rate constants) and stabilities of the yielded **CA•** radicals. As for the RAF mechanism, double bond of the conjugate chain (more precisely C8) is the preferred site of **CA** for HO• binding. This pathway requires the lowest activation energy and yields the most stable radical adduct. Electrophilic C9 of the carboxyl group is not a favoured position for HO• binding.

ET from **CA** to HO• is endergonic and requires enormously large activation energies in both solvents. These facts designate SET-PT as an implausible antioxidative mechanism of **CA**. In basic environment formation of phenolate **CA⁻** anions is facilitated. ET from **CA⁻** to HO• in water solution is a diffusion controlled reaction. The so-formed hydroxide anions propagate the chain reaction.

In conclusion: HAT and RAF are competitive antioxidative mechanisms of **CA**, because HAT pathways yield thermodynamically more stable radical products, and RAF pathways require smaller activation barriers. In polar basic environment SPLET is a probable antioxidative mechanism of **CA**, with extremely large rate. The results of our investigation are in relatively good accord with those obtained from the gas-phase computations [19]. Our findings agree very well with the experimental results related to the rate constant for the reaction of **CA** with HO• (KONO *et al.*, 1997).

Acknowledgments

This work was supported by the Ministry of Science and Technological Development of the Republic of Serbia (project no 172016).

References:

[1] BELITZ, H.D., GROSCH, W., SCHIEBERLE, P. (2009): *Food chemistry.* Berlin: Springer-Verlag.

[2] CHALLIS, B.C., BARTLETT, C.D. (1975): Possible cocarcinogenic effects of coffee constituents, *Nature* **254**: 532–533.

[3] COLLINS, F.C., KIMBALL, G.E. (1949): Diffusion-controlled reaction rates, *J. Colloid Sci.* **4**: 425–437.

[4] COSSI, M., REGA, N., SCALMANI, G., BARONE, V. (2003): Energies, structures, and electronic properties of molecules in solution with the C-PCM solvation model, *J. Comput. Chem.* **24**: 669–681.

[5] EINSTEIN, A. (1905): Über die von der molekularkinetischen Theorie der Wärme gefordete Bewegung von in ruhenden Flüssigkeiten suspendierten Teilchen, *Ann. Phys.* **17**: 549–560.

[6] EVANS, M. G., POLANYI, M. (1935): Some applications of the transition state method to the calculation of reaction velocities, especially in solution, *Trans. Faraday Soc.* **31**: 875–894.

[7] EYRING, H. (1935): The activated complex in chemical reactions, *J. Chem. Phys*. **3**: 107–115.

[8] FRANK, H., THIEL, D., MACLEOD, J. (1989): Mass spectrometric detection of cross-linked fatty acids formed during radical-induced lesion of lipid membranes, *Biochem. J.* **260**: 873–878.

[9] FRISCH, M.J., TRUCKS, G.W., SCHLEGEL, H.B., SCUSERIA, G.E., ROBB, M.A., CHEESEMAN, J.R., SCALMANI, G., BARONE, V., MENNUCCI, B., PETERSSON, G.A. et al. (2013): *Gaussian 09, Revision D.1*. Wallingford CT: Gaussian Inc.

[10] GALANO, A., ALVAREZ-IDABOY, J.R. (2013): A computational methodology for accurate predictions of rate constants in solution: Application to the assessment of primary antioxidant activity, *J. Comput. Chem.* **34**: 2430–2445.

[11] GALANO, A., MAZZONE, G., ALVAREZ-DIDUK, R., MARINO, T., ALVAREZ-IDABOY, J. R., RUSSO, N. (2016): The food antioxidants: Chemical insights at the molecular level, *Annu. Rev. Food Sci. T.* **7**: 335–352.

[12] GEBHARDT, R., FAUSEL, M. (1997): Antioxidant and hepatoprotective effects of artichoke extract and constituents in cultured rat hepatocytes, *Toxicology* **11**: 669–672.

[13] GONZÁLEZ MOA, M.J., MANDADO, M., MOSQUERA, R.A. (2006): QTAIM charge density study of natural cinnamic acids, *Chem. Phys. Lett.* **424**: 17–22.

[14] IWAHASHI, H., ISHII, T., SUGATA, R., KIDO, R. (1990): The effects of caffeic acid and its related catechols on hydroxyl radical formation by 3-hydroxyanthranilic acid, ferric chloride, and hydrogen peroxide, *Arch. Biochem. Biophys.* **276**: 242–247.

[15] JOYEUX, M., LOBSTEIN, A., ANTON, R., MORTIER, F. (1995): Comparative antilipoperoxidant, antinecrotic ans scavenging properties of terpenes and biflavones from Ginkgo and some flavonoids, *Planta Med.* **61**: 126–129.

[16] KLEIN, E., LUKEŠ, V., ILČIN, M. (2007): DFT/B3LYP study of tocopherols and chromans antioxidant action energetics, *Chem. Phys.* **336**: 51–57.

[17] KONO, Y., KOBAYASHI, K., TAGAWA, S., ADACHI, K., UEDA, A., SAWA, Y., SHIBATA, H. (1997): Antioxidant activity of polyphenolics in diets. Rate constants of reactions of chlorogenic acid and caffeic acid with reactive species of oxygen and nitrogen, *Biochim. Biophys. Acta* **1335**: 335–342.

[18] LENTE, G. (2015): *Deterministic kinetics in Chemistry and systems biology*. Cham: Springer.

[19] LEOPOLDINI, M., CHIODO, S. G., RUSSO, N., TOSCANO, M. (2011): Detailed investigation of the OH radical quenching by natural antioxidant caffeic acid studied by quantum mechanical models, *J. Chem. Theory Comput.* **7**: 4218–4233.

[20] LITWINIENKO, G., INGOLD, K.U. (2007): Solvent effects on the rates and mechanisms of reaction of phenols with free radicals, *Accounts Chem. Res.* **40**: 222–230.

[21] MARCUS, R.A. (1993): Electron transfer reactions in chemistry. Theory and experiment, *Rev. Mod. Phy.* **65**: 599–610.

[22] MARKOVIĆ, S., TOŠOVIĆ, J. (2016): Comparative study of the antioxidative activities of caffeoylquinic and caffeic acids, *Food Chem.* **210**: 585–592.

[23] MARTÍNEZ, A., HERNÁNDEZ-MARTIN, E., GALANO, A. (2012): Xanthones as antioxidants: A theoretical study on the thermodynamics and kinetics of the single electron transfer mechanism, *Food Funct.* **3**: 442–450.

[24] MILENKOVIĆ, D., TOŠOVIĆ, J., MARKOVIĆ, S., MARKOVIĆ, Z. (2016): Reakcije prelaza elektrona: Markusova teorija, *Hem. pregled* **57**: 92–97.

[25] NELSEN, S.F., BLACKSTOCK, S.C., KIM, Y. (1987): Estimation of inner shell Marcus terms for amino nitrogen compounds by molecular orbital calculations, *J. Am. Chem. Soc.* **109**: 677–682.

[26] NELSEN, S.F., WEAVER, M.N., LUO, Y., PLADZIEWICZ, J.R., AUSMAN, L.K., JENTZSCH T.L., O'KONEK, J.J. (2006): Estimation of electronic coupling for intermolecular electron transfer from cross-reaction data, *J. Phys. Chem. A.* **110**: 11665–11676.

[27] SMOLUCHOWSKI, M.V. (1917): Versuch einer mathematischen Theorie der Koagulationskinetik kolloider Lösungen, *Z. Phys. Chem.* **92**: 129–168.

[28] STOKES, G.G. (1901): *Mathematical and Physical Papers*. Cambridge: Cambridge University Press.

[29] SUDINA, G.F., MIRZOEVA, O.K., PUSHKAREVA, M.A., KORSHUNOVA, G.A., SUMBATYAN, N.V., VARFOLOMEEV, S.D. (1993): Caffeic acid phenethyl ester as a lipoxygenase inhibitor with antioxidant properties, *FEBS Lett.* **329**: 21–24.

[30] TRUHLAR, D.G. (1985): Nearly encounter-controlled reactions: The equivalence of the steady-state and diffusional viewpoints, *J. Chem. Educ.* **62**: 104–106.

[31] TRUHLAR, D.G., HASE, W.L., HYNES, J.T. (1983): Current status of transition-state theory, *J. Phys. Chem.* **87**: 2664–2682.

[32] WRIGHT, J.S., JOHNSON, E.R., DILABIO, G.A. (2001): Predicting the activity of phenolic antioxidants: Theoretical method, analysis of substituent effects, and application to major families of antioxidants, *J. Am. Chem. Soc.* **123**: 1173–1183.

[33] XU, J.G., HU, Q.P., LIU, Y. (2012): Antioxidant and DNA-protective activities of chlorogenic acid isomers, *J. Agric. Food Chem.* **60**: 11625–11630.

[34] ZHAO, Y., TRUHLAR, D. G. (2008): Density functionals with broad applicability in chemistry, *Acc. Chem. Res.* **41**: 157–167.

[35] http://www.trimen.pl/witek/ciecze/liquids.html Accessed 27 December 2016.